Environmental Research 294 (2026) 123825

Contents lists available at ScienceDirect

Environmental Research

journal homepage: www.elsevier.com/locate/envres

Meso- and microplastics accumulate and transfer hazardous contaminants from wastewater treatment plants to the environment

Simone Cavazzoli [a,*], Marie Morere [b], Gianni Andreottola [a], Mathilde Monperrus [b]

[a] Department of Civil, Environmental and Mechanical Engineering, University of Trento, Via Mesiano 77, Trento, 38123, Italy
[b] Université de Pau et des Pays de l'Adour, E2S UPPA, CNRS, IPREM-MIRA, UMR 5254, Anglet, 64600, France

ARTICLE INFO

Keywords:
Contaminant of emerging concern
Priority pollutant
Adsorption
Polymer
Daily flux

ABSTRACT

The ubiquitous presence of meso- and microplastics (M-MPs) in aquatic systems, together with their capacity to act as vectors for contaminants, poses growing concerns for ecosystem and human health. Municipal wastewater treatment plants (WWTPs) play a dual role, partially mitigating but also redistributing M-MPs through effluent discharge and sludge management. This study investigated the association of M-MPs with organic and inorganic micropollutants, including metal(loid)s, synthetic musk fragrances (SMFs), UV filters, pharmaceuticals, organophosphate flame retardants, and pesticides, across WWTP streams. Contaminant partitioning between suspended particulate matter (SPM) and the dissolved phase was evaluated in influent and effluent, and dewatered sludge was also assessed. Results indicated relevant emissions of metal(loid)s, SMFs, and UV filters *via* treated wastewater. In the effluent, hydrophobic compounds were mostly associated with SPM, while hydrophilic compounds remained predominantly dissolved. M-MPs carried measurable pollutant loads per unit mass, with polystyrene microspheres (500–1000 μm) exhibiting the highest concentrations among the polymers analyzed, reaching 5.2 mg/kg for pharmaceuticals, 283.7 mg/kg for SMFs, and 991.5 mg/kg for UV filters—values comparable to those found on bulk SPM in this study. However, because of their lower abundance, polystyrene particles contributed less to the overall micropollutant flux than polyethylene and polypropylene, which dominated the discharged plastic mass. These results show that M-MPs, as a component of the suspended particulate fraction, constitute a relevant pathway for micropollutant transport in WWTP effluents and underline the need for size-inclusive monitoring and advanced treatment technologies to limit environmental releases.

1. Introduction

Microplastics (MPs), commonly defined as plastic particles and fibers smaller than 5 mm in diameter, have become pervasive contaminants in both terrestrial and marine environments (UNEP, 2021). Ubiquitous across oceans, rivers, soils and even the atmosphere, MPs threaten biodiversity and disrupt ecosystem processes (Osman et al., 2023; Triebskorn et al., 2019). Wastewater treatment plants (WWTPs) represent a critical control point for MP inputs: although not explicitly engineered for MPs removal, conventional treatment processes nonetheless retain a substantial portion of incoming MPs by sequestering them in sewage sludge (Rout et al., 2022). Yet, given the vast volumes of effluent discharged daily, WWTPs continue to serve as major conduits for MPs into aquatic systems (Niari et al., 2023). Understanding not only their removal efficiency but also their transformation and fate within WWTPs is essential for assessing both downstream aquatic impacts and land-based exposure routes through biosolid application.

Despite their direct toxicity to aquatic and terrestrial organisms, MPs released in the environment pose even greater risks by serving as vectors for a wide array of wastewater-borne contaminants. Owing to their minute size and high surface-area-to-volume ratio, MPs efficiently adsorb both potentially hazardous trace elements (PHTEs) and organic compounds, including priority pollutants and a diverse suite of contaminants of emerging concern (CECs) such as pharmaceutical compounds (PCs), per- and polyfluoroalkyl substances, endocrine disruptors, viruses, and antimicrobial-resistance markers (Acarer, 2023; Kumar et al., 2021). Unlike conventional pollutants, most CECs remain unregulated, heightening worries over their persistence and bioaccumulation in food webs (Parida et al., 2021; Petrie et al., 2015). In response, the EU has adopted Directive (EU) 2024/3019, which mandates harmonized

This article is part of a special issue entitled: Microplastics as carriers: risks to human health published in Environmental Research.

* Corresponding author.
E-mail address: simone.cavazzoli@unitn.it (S. Cavazzoli).

https://doi.org/10.1016/j.envres.2026.123825
Received 2 September 2025; Received in revised form 6 January 2026; Accepted 19 January 2026
Available online 19 January 2026

monitoring methods and requires at least 80 % removal of a proxy group of micropollutants *via* quaternary treatment, but leaves specific discharge limits and the choice of abatement technologies to Member States and future Commission implementing acts (EU, 2024). Common CECs in wastewater include PCs, personal care products, flame retardants, pesticides, and various industrial chemicals (Pastorino and Ginebreda, 2021). Many of these compounds bioaccumulate and biomagnify through food webs, causing neurological impairments, reproductive dysfunctions, behavioural alterations, and endocrine disruption in aquatic organisms (Bexfield et al., 2019; Blum et al., 2019; Cao et al., 2014; Li et al., 2016). Organic CECs can be grouped by hydrophobicity using their octanol–water partition coefficient (K_{ow}): contaminants with Log $K_{ow} > 3$ are considered hydrophobic (Teuten et al., 2007). For example, synthetic musk fragrances (SMFs) and UV-filters (UV-f) are typically hydrophobic, whereas PCs, pesticides, and organophosphate flame retardants (OPFRs) tend to be more hydrophilic. In addition to K_{ow}, factors such as aqueous solubility, volatility, pH, ionic strength, and organic matter (OM) content govern how these compounds partition in the environment and interact with biota (Mackay and Clark, 1991).

When it comes to micropollutant adsorption, hydrophobic contaminants tend to associate with the intact, nonpolar surfaces of pristine polymers, whereas hydrophilic or polar compounds bind more readily to charged or weathered surfaces, including those enriched with OM, biofilms or colloids, through electrostatic attraction and hydrogen bonding (Agboola and Benson, 2021; J. Wang et al., 2019). The sorptive behaviour of MPs is thus strongly governed by polymer composition, surface functionality and the physicochemical conditions of wastewater (Acarer, 2023; Titov et al., 2024; Fu et al., 2021). As polymeric surfaces age, they undergo oxidation, abrasion and photo-degradation, resulting in increased surface roughness and the introduction of oxygen-containing functional groups. These changes enhance sorption capacity and alter the types of interactions that can occur with dissolved contaminants (Al-Mamun et al., 2019). A further layer of complexity arises from the ecocorona, a dynamic coating of organic and inorganic material that rapidly forms on MPs in aquatic environments (Yang et al., 2025). The ecocorona can profoundly reshape particle behavior by modifying surface charge, hydrophobicity and the availability of binding sites, ultimately altering the sorption of environmental contaminants (Amaral-Zettler et al., 2020; Kopatz et al., 2023). Corona constituents such as polysaccharides, proteins, humic substances and extracellular polymeric substances can either promote or inhibit micropollutant sorption depending on their chemical characteristics (Galloway et al., 2017). For example, humic and fulvic acids may enhance sorption of hydrophobic contaminants by increasing surface hydrophobicity and introducing additional aromatic moieties (Dong et al., 2020), whereas protein-rich coronas can introduce steric hindrance or compete with pollutants for surface sites (Schvartz et al., 2023). The ecocorona also mediates interactions with biota, influencing ingestion, assimilation, immune response, biodeposition and toxicity (Schwabl et al., 2019; Zimmermann et al., 2019), and may act as a carrier for additional contaminants associated with biofilms, including trace metals, pharmaceuticals and pathogens (Richard et al., 2019; Stabnikova et al., 2022).

Despite these advances, most existing knowledge still derives from controlled laboratory systems or artificially aged plastics, whereas far fewer studies have characterized the contaminant mixtures associated with environmentally weathered MP particles collected directly from operational WWTPs. A key knowledge gap therefore concerns the actual suite of micropollutants associated with environmental MPs released into the environment, and the relative contribution of different polymers to their transport. WWTPs discharge both hydrophilic and hydrophobic contaminants alongside diverse MP assemblages (Cavazzoli et al., 2023; Stroski, 2019), yet quantifying how these pollutants partition between suspended solids, dissolved phases and specific polymer types remains limited. To address this knowledge gap, we (1) identify and quantify organic and inorganic micropollutants associated with M-MPs recovered directly from WWTP effluent; (2) determine how different chemical classes and polymer types preferentially associate under real wastewater conditions; and (3) estimate the daily fluxes of these micropollutants transported *via* plastics. In parallel, we quantify contaminant loads in influent, effluent and biosolids to construct a mass balance of removal and release, partitioning each compound between dissolved and particulate phases. This integrated approach provides a polymer-resolved assessment of micropollutant transport by environmentally aged M-MPs and clarifies their contribution within the overall contaminant pathways of a conventional WWTP.

2. Materials and methods

2.1. Description of the WWTP

The WWTP studied is situated on France's southwestern coast and is fed by three main urban pumping stations. It is designed for 112,000 population equivalent and operates two parallel treatment trains, processing on average 23,000 m^3 of wastewater per day and treating roughly 6700 kg of biological oxygen demand (BOD_5) daily. Treatment begins with enclosed static pre-treatment (screening, degritting, and degreasing) to remove coarse solids and grit and to control odours. Primary settling in lamellar clarifiers then removes ~60 % of sedimentable solids and ~30 % of BOD_5. The biological stage employs conventional activated sludge with nitrification and denitrification for nitrogen removal; phosphorus removal is not implemented. Following secondary clarification, effluent is discharged into the Adour River. A process flow diagram is provided in Supplementary Figure S1.

2.2. Sampling and sample preparation

2.2.1. Influent, effluent, and sludge samples

Sampling was performed under semi-dry weather conditions. Twenty-four-hour composite influent and effluent samples were collected with stationary autosamplers (Hach Lange, USA); the effluent was sampled 27 h after the influent to match the plant's hydraulic retention time (HRT, see Supplementary Fig. S2). Samples were transferred immediately into filled amber glass bottles to minimize headspace, kept at 4 °C, and analyzed within 72 h for both dissolved and total solid pollutant fractions. To quantify the total micropollutant concentrations in the influent and effluent wastewaters, comprising the solid particulate material (SPM) fraction (C_{SPM}) and the dissolved fraction (C_{DISS}), 2 L samples were collected. Aliquots of these volumes (~200 mL) were filtered using 0.45 μm filters, with cellulose acetate filters employed for organic contaminants and PVDF filters for inorganic contaminants. Filtration blanks using Milli-Q water were prepared for each contaminant type analyzed, including metals and metalloids, hydrophobic organic contaminants, and hydrophilic organic contaminants. Following filtration, the filters were stored at −20 °C for C_{SPM} analysis, while the filtrates (C_{DISS}) were refrigerated at +4 °C until further analysis. The filtrates of metal(loid)s were treated with 1 % v/v HNO_3. Biosolid sample, consisting in 250 g of mixed primary and floated activated sludge dewatered by centrifugation, was collected in a glass beaker, aliquoted into 50 mL tubes, and stored at −20 °C. A representative 40 g subsample was freeze-dried for 72 h. The resulting lyophilized sludge was ground to a fine powder using a pre-cleaned glass pestle and mortar, then returned to −20 °C storage until chemical extraction.

2.2.2. M-MPs samples

To collect sufficient plastic material from WWTP effluent for chemical extraction and mass-spectrometric analysis, we employed an *in-situ* pump-and-filtration system consisting of two peristaltic pumps (PD5206, Heidolph, Germany). The pumps operated continuously for 24 h at a flow rate of 750 mL min^{-1} each, drawing effluent through a cascade of stainless-steel sieves (Endecotts, UK) with mesh sizes of 5000, 1000, 500, and 300 μm. This setup processed approximately 2160 L of

effluent per sampling event. In total, eleven 24-h sessions were carried out under semi-dry weather conditions over a period of 1.5 months, resulting in a cumulative volume of 22,680 L of effluent filtered. Throughout the sampling campaign, WWTP operational conditions, including wastewater flow rate and treatment efficiency, remained stable and comparable. To minimize algal fouling, each suction inlet was fitted with a 5 mm cylindrical screen mesh. At the end of each session, the sieves were sealed and transported to the laboratory, where retained material was gently back-washed onto the finest (300 μm) sieve using tap water. The concentrated solids were then transferred into pre-cleaned Petri dishes and refrigerated (4 °C) for up to 24 h before microscopic sorting. Effluent filtration also captured plastic fragments between 5000 and 10,000 μm; accordingly, our analysis encompasses M-MPs which are plastic particles up to 20 mm in size (Debroy et al., 2022).

The retained solids were initially inspected under a stereomicroscope (Advance ICD, Bresser, Germany) to document particle morphology (shape, size, and colour) and to identify potential plastic candidates. To preserve micropollutants adsorbed onto particle surfaces, no chemical purification was applied prior to analysis. Particle selection was therefore based on predefined visual and mechanical criteria, following the approach described by Markley et al. (2024). Particles exhibiting clearly organic or cellular structures, such as plant debris or wood fragments, were excluded. Candidate particles were required to withstand gentle mechanical pressure applied with metal tweezers, thereby eliminating friable or easily deformable organic material. Selection further focused on particles displaying visual features inconsistent with the surrounding matrix, including uniform or artificial coloration, regular or angular morphology, and surface textures characteristic of synthetic polymers. Representative optical images and the corresponding ATR-FTIR spectra used to confirm polymer identity are provided in Supplementary Fig. S3–S13 to support transparency and reproducibility. Identified M-MPs were classified into five morphological categories: spheres, films, granules, fibers, and fragments (Markley et al., 2024). Each putative M-MP (N = 350) was then transferred into an individual well of a 96-well plate for polymer identification by attenuated total reflection Fourier-transform infrared spectroscopy (ATR-FTIR; Nicolet iS20, Thermo Scientific, USA). Spectra were acquired over 4000–450 cm^{-1} at 4 cm^{-1} resolution, with 64 co-added scans per sample. Before each batch, the ATR diamond crystal was wiped with acetone and a fresh background spectrum collected. Sample spectra were automatically matched against the Thermo Scientific polymer library using the software's peak-finding algorithms to confirm polymer type *via* diagnostic absorption bands.

Since no chemical purification was performed, thereby preserving adsorbed pollutants, only ATR-FTIR spectra with a library match score $\geq$0.70 were accepted outright as reliable identifications. Although this threshold might appear low, it was selected because many M-MPs were still covered by a thin but persistent layer of OM (eco-corona), which often prevented the acquisition of high-quality FTIR spectra. Nevertheless, in the spectral identification software, the assigned polymer consistently represented the highest-probability match, with a markedly greater score than subsequent alternatives. In some cases, rotating the particle and thereby changing the IR incidence angle yielded spectra that confirmed the polymer identity with substantially improved quality. Another factor influencing the match score is the degree of plastic degradation (Singh and Sharma, 2008), which in this study can be considered high given the investigated matrix. For spectra with match scores between 0.60 and 0.69, diagnostic absorption bands were manually inspected (Jung et al., 2018): particles exhibiting the characteristic peaks were retained, whereas those without were discarded, in accordance with Yang et al. (2015). All retained particles also displayed visual features consistent with plastic origin (e.g., irregular but blocky morphology, bright coloration). Spectra scoring <0.60 were excluded (Yang et al., 2015). Polyethylene (PE) dominated the effluent M-MPs assemblage, followed by polypropylene (PP) and polystyrene (PS). Less abundant polymers, i.e., nylon-6, PE/PP copolymers, EVA, and polydimethylsiloxane (PDMS), were grouped as "Other." After FTIR confirmation, particles were pooled by polymer category and weighed, yielding 323.0 mg of PE, 197.7 mg of PP, 3.1 mg of PS, and 9.8 mg of other polymers. The mass of adhered biofilm and associated OM was not separated from the polymer mass prior to weighing. Accordingly, environmentally aged MPs were treated as integrated plastic–ecocorona systems. This approach was adopted to preserve micropollutant associations and to reflect realistic environmental conditions in wastewater effluents. Available literature indicates that biofilm and organic coatings generally contribute a minor, though variable, fraction of the total particle mass—often on the order of a few percent under environmental conditions, with values depending on polymer type, exposure duration, and matrix characteristics (Gavlová et al., 2025; Rummel et al., 2017). Consequently, the reported concentrations represent micropollutant loads normalized to the mass of environmentally aged MPs complexes rather than pristine polymer material. Each polymer pool was subsequently subdivided for micropollutant extraction, allocating 20 % of the mass for metal(loid) analysis, 40 % for hydrophobic organic micropollutants, and 40 % for hydrophilic organic micropollutants. Due to limited sample mass, further subdivision for analytical replicates was not feasible.

2.3. Chemical extraction and instrumental analysis

2.3.1. Metals and metalloids

For the analysis of metals and metalloids in the M-MPs fraction, an aliquot corresponding to one-fifth of the total mass of each polymer pool was accurately weighed and transferred into 15 mL plastic vials. Subsequently, 2 mL of 70 % analytical-grade HNO_3 were added, and the vials were placed in a hot block (DigiPrep Jr, SCP Science, Canada) at 85 °C for 30 min. This limited digestion time was chosen to prevent the degradation of more fragile polymers, such as nylons. Three extraction blanks (HNO_3 and Milli-Q water) were processed in parallel with the samples. After digestion, the acid extracts were quantitatively transferred into new 15 mL vials and brought to volume with Milli-Q water. The same sample preparation procedure was applied to the filters used for SPM analysis (influent, effluent, and filtration blanks) and to the sludge samples. For the dissolved contaminant fraction (influent, effluent, and filtration blanks), 15 mL of pre-filtered and acidified solutions (see paragraph 2.2.1) were directly transferred into plastic vials. All prepared samples were stored at +4 °C until analysis by inductively coupled plasma mass spectrometry (ICP-MS, Agilent 7500, Agilent Technologies, USA). Instrument control, data acquisition, and processing were conducted using Agilent Chemstation software. Detection (LOD) and quantification (LOQ) limits for major and trace elements, as well as organic micropollutants, are provided in Supplementary Table S3. In parallel, procedural blanks were systematically included for all micropollutant analyses and processed using the same extraction, filtration, and analytical procedures as the samples, allowing correction for background contamination originating from reagents, laboratory environment, and sample handling.

2.3.2. Hydrophobic contaminants (synthetic musks and UV-filters)

For the extraction of hydrophobic organic contaminants from solid matrices, the analysis targeted common SMFs and UV-f using the method described by Elseblani et al. (2023). This methodology was applied to M-MPs collected from the effluent, filters used for SPM analysis, and sludge samples. Each sample was carefully transferred into a 15 mL glass vial. A 6 mL mixture of dichloromethane (DCM) and hexane (HEX) in a 1:1 ratio was then added, along with the internal standard (IS), deuterated Musk xylene (MX D15), at a final concentration of 10 μg/L. The vials were placed in an ultrasonic cleaner (USC) for 10 min to facilitate extraction. The first extract was recovered into a clean glass vial, while the original sample was subjected to a second extraction with 6 mL of isooctane, again in the USC for 10 min. Both extracts (approximately 12 mL total) were then combined and

concentrated to dryness using a solvent evaporator (TurboVap LV, Biotage, Sweden). The resulting residue was reconstituted in 0.5 mL of isooctane and transferred into GC vials for analysis. Due to their higher analyte concentrations, sludge extracts were reconstituted in 4 mL of isooctane instead of 0.5 mL. A 1 mL aliquot of this reconstituted solution was filtered through a 0.2 μm cellulose acetate syringe filter directly into GC vials for analysis.

For the analysis of the dissolved fraction, the method described by Cavalheiro et al. (2017) was followed (Cavalheiro et al., 2017). A 100 mL aliquot of the sample was transferred into a 150 mL glass bottle, to which 10 μL of the IS (MX D15) were added to achieve a final concentration of 1 ppm. Three hollow polyether sulfone (PES) tubes, each 1 cm in length, were also added to the bottle to adsorb and concentrate dissolved organic contaminants. The bottle was covered with aluminum foil to prevent photodegradation and agitated for 5 h. After this contact time, the PES tubes were transferred into Eppendorf tubes containing 1 mL of isooctane. The tubes were placed in an USC for 10 min to desorb the contaminants. The resulting isooctane solution was then transferred into GC vials for analysis.

Samples were analyzed using a Trace 1600 Gas Chromatograph coupled with an ISQ 7610 Mass Spectrometer (GC/MS) equipped with an Electron Ionization (EI) source and a split/splitless injector (Thermo Fisher Scientific, USA). The GC/MS system featured a split/splitless focus liner packed with glass wool and a TraceGOLD TG-5MS capillary column (15 m length × 0.25 mm internal diameter × 0.25 μm film thickness). Helium (He), with a purity greater than 99.9 % (Linde), was used as the carrier gas. Optimized analytical parameters for GC/MS analysis are provided in **Supplementary Text 1** (GC/MS), while the detection parameters and IS used for individual micropollutants are detailed in Supplementary Table S1. Instrument control, data acquisition, and processing were carried out using Chromeleon software (v. 7.3.2). Quantification was performed in Selected Ion Monitoring (SIM) mode, using two characteristic fragment ions per compound: one Target ion for quantification and one Qualifier ion for confirmation.

2.3.3. Hydrophilic contaminants (pharmaceuticals, flame retardants, pesticides)

For the analysis of hydrophilic organic contaminants in the various samples (influent, effluent, sludge, and M-MPs), the study targeted several PCs, OPFRs, and pesticides. The extraction method for M-MPs collected from the effluent, filters used for SPM analysis, and sludge samples was adapted from Miossec et al. (2019). Each sample was carefully transferred into a 15 mL glass vial, followed by the addition of 5 mL of an acetonitrile (ACN) and MeOH mixture (1:1, v/v). IS were added to reach final concentrations of 20 ppb for PCs and 10 ppb for both OPFRs and pesticides. The vials were placed in an USC for 10 min. The first extract was transferred into a clean glass vial, and a second extraction was performed using an additional 5 mL of the ACN:MeOH mixture under the same conditions. The two extracts (approximately 10 mL total) were then combined and evaporated to dryness using a solvent evaporator. The residue was reconstituted in 1 mL of a Milli-Q water: MeOH solution (0.75:0.25, v/v), acidified with 0.1 % formic acid. This solution was transferred into LC vials for analysis. As with hydrophobic contaminants, sludge samples showed high concentrations of organics. Therefore, dried sludge extracts were reconstituted in 10 mL of the acidified Milli-Q water:MeOH solution. A 1 mL aliquot was filtered through a 0.2 μm cellulose acetate syringe filter and transferred into LC vials for injection.

For the analysis of the dissolved fraction in aqueous samples, a 20 mL aliquot was transferred into a glass vial. IS for PCs, OPFRs, and pesticides were added to achieve final concentrations of 10, 20, and 10 ppb, respectively. The solution was then processed through a solid-phase extraction (SPE) cartridge (Oasis, Waters, USA), previously conditioned with 3 mL of MeOH followed by 3 mL of Milli-Q water. After analyte retention on the SPE cartridge, elution was performed using two successive 3 mL portions of MeOH. The combined eluate was collected in a clean glass vial, evaporated to dryness, and reconstituted in 1 mL of MeOH. The final solution was transferred into LC vials for analysis by LC-MS^2.

Liquid chromatographic analyses were performed using an Acquity UPLC system coupled to a Xevo TQ MS triple quadrupole mass spectrometer with an electrospray ionization (ESI) source (Waters, USA). Chromatographic separation was achieved using an Acquity UPLC HSS T3 column (1.8 μm particle size, 50 mm × 2.1 mm i.d.), preceded by a guard column of the same particle size (5 mm × 2.1 mm i.d.). Optimized analytical parameters for LC/MS^2 analysis are provided in **Supplementary Text S2** (LC/MS^2), while detection settings and the IS used for individual micropollutants are detailed in Supplementary Table S2. Instrument control, data acquisition, and processing were performed using MassLynx software. Quantification was carried out in Multiple Reaction Monitoring (MRM) mode, with two characteristic transitions selected for each compound (Miossec et al., 2019).

3. Results

3.1. M-MPs in the WWTP effluent

The number, physical characteristics (shape and size), and polymer types of M-MPs collected at the investigated WWTP are presented in Fig. 1. A total of 160 particles with spectra of sufficient quality were identified by ATR-FTIR. The concentration of M-MPs detected in the effluent was relatively low (0.07 M-MPs L^{-1}, corresponding to approximately one particle per 140 L of filtered water), which can be attributed to several methodological and process-related factors. First, the analysis was restricted to particles larger than 300 μm. Excluding smaller size fraction inevitably leads to an underestimation of the total MPs-associated micropollutant load and, more importantly, of the total surface area available for adsorption. Smaller MPs are typically far more abundant than larger particles in WWTPs (Ali et al., 2021), whereas larger plastics are preferentially removed during coagulation, flocculation, and sedimentation processes and become incorporated into sludge flocs (Rout et al., 2022). Moreover, the specific surface area of particulate solids, including MPs, increases markedly with decreasing particle size, further amplifying the potential contribution of the <300 μm fraction to contaminant sorption. Second, no chemical purification was applied prior to particle selection, which limited particle recovery, as untreated effluent contains a complex organic matrix that hinders the visual detection and isolation of plastics (Nguyen et al., 2019). The high abundance of filamentous algae in the samples further prevented reliable quantification of most M-MP fibers, which are known to represent a substantial fraction of WWTP M-MPs emissions. Although purification steps are commonly employed to improve particle separation and analytical robustness (Cavazzoli et al., 2023; Cavazzoli et al., 2025a,b), they were intentionally omitted in this study to preserve micropollutants adsorbed onto particle surfaces and to maintain the integrity of the eco-corona (Amaral-Zettler et al., 2020). Instead, particles were gently rinsed with tap water. This methodological choice reflects the primary aim of the study, which was not to quantify M-MPs abundance in the effluent, but to identify priority pollutants and CECs associated with environmentally aged M-MPs and to assess polymer-specific sorption patterns under realistic wastewater conditions.

Microscopical observation of separated M-MPs revealed white as the most common colour, followed by transparent, black, red, blue, grey, and green. Smaller numbers of yellow, orange, and fuchsia particles were also detected. PE was the dominant polymer, representing 42 % of the total, mainly as fragments and fibers ranging from 2500 to 5000 μm. PP accounted for 28 %, with most particles between 1000 and 5000 μm, predominantly in fragment and fiber form. PS comprised 23 %, occurring primarily as spherical particles in the 500–1000 μm range. The remaining 7 % were classified as “Other” (Fig. 1), largely fragments. Representative ATR-FTIR spectra for each polymer category (PE, PP, PS, and “Other”), together with corresponding optical images, are shown in

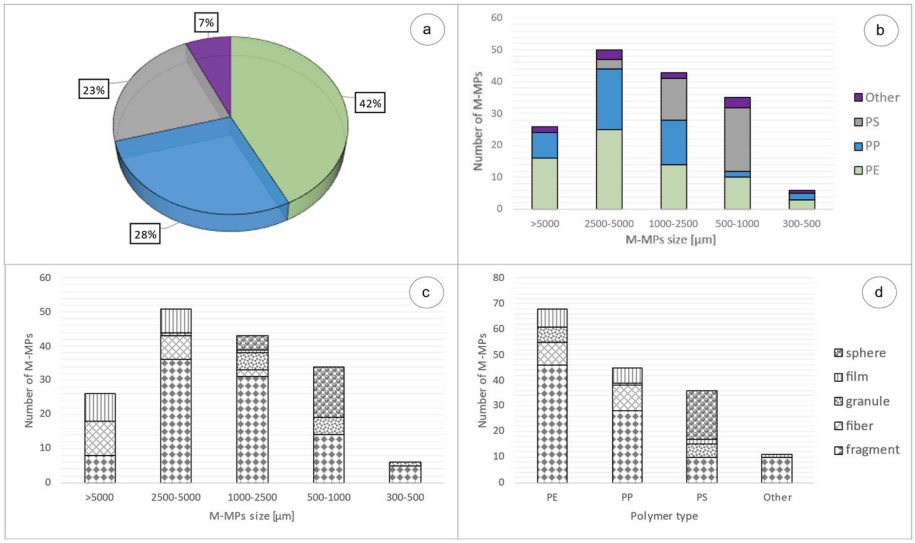

Fig. 1. Graphical summary of meso- and microplastics found in WWTP effluent. a) composition (N, %) of polymers found in the overall samples; b) size distribution of polymers; c, d) size and polymer distribution of M-MPs according to their shape (sphere, film, granule, fiber, fragment).

Supplementary Fig. S3–S13. Based on the average outflow rate of approximately 23,000 m^3 day^{-1} during the sampling period, the daily release of M-MPs into the receiving water body was estimated. Since identified M-MPs were weighed after air-drying for 48 h, the corresponding daily polymer mass discharged by the plant was also calculated. These estimates should, however, be interpreted with caution given the study limitations discussed above and are likely conservative estimates of M-MP emissions. The results indicate that 162,257 M-MPs are released daily into the aquatic environment *via* the effluent of the investigated WWTP. Of these, 68,148 particles are PE, 45,432 are PP, 37,319 are PS, and 11,358 fall under the "Other" category, which includes nylon, PE/PP copolymers, EVA, and PDM. In terms of mass, the total detected concentration of M-MPs corresponds to 23.5 µg/L, resulting in an estimated 542 g of M-MPs discharged daily. This includes 227 g day^{-1} of PE, 152 g day^{-1} of PP, 124 g day^{-1} of PS, and 38 g day^{-1} from the "Other" category. When comparing these results to literature data, it becomes evident that other studies have reported substantially higher numbers of MP particles in WWTP effluents, often several orders of magnitude greater than those observed here (Iordachescu et al., 2024; Pagliaccia et al., 2025). These discrepancies are likely attributable to differences in sampling strategies, particle size detection limits, and analytical methodologies. A similar trend is observed in mass-based assessments. In a previous study conducted by our research group, the concentration of common MP polymers in WWTP effluents, down to 2 µm in size and quantified *via* thermal desorption gas chromatography–mass spectrometry, ranged from 215 µg/L to 761 µg/L, depending on the plant investigated and the specific wastewater treatment technology employed (Cavazzoli et al., 2025a).

3.2. Organic and inorganic contaminants exiting the WWTP via M-MPs

3.2.1. Major- and trace elements

For clarity in reporting, metals and metalloids detected on M-MPs were categorized as major elements (Al, Fe, Zn, Cu, B, Ba) or trace elements (Cd, Cr, Mn, Ni, Pb, Ag, As, Co, Hg, Mo, Sb, Sn, V), based on their relative abundance in the samples. Fig. 2 presents the concentrations of these elements detected on M-MPs, expressed in mg per kg of polymer on a dry weight (dw) basis. Detailed numerical values are provided in Supplementary Tables S4 and S5. Standard deviations reported for ICP-MS measurements reflect instrumental repeatability (i.e., replicate injections). Among the major elements, iron, aluminum, and zinc were consistently the most abundant across all polymer types. Notably, PS exhibited concentrations approximately an order of magnitude higher than those observed for other polymers. For example, PS carried 46.8 ± 0.05 mg/kg of copper and 37.3 ± 0.1 mg/kg of manganese. A similar pattern was observed for trace elements: PS particles consistently

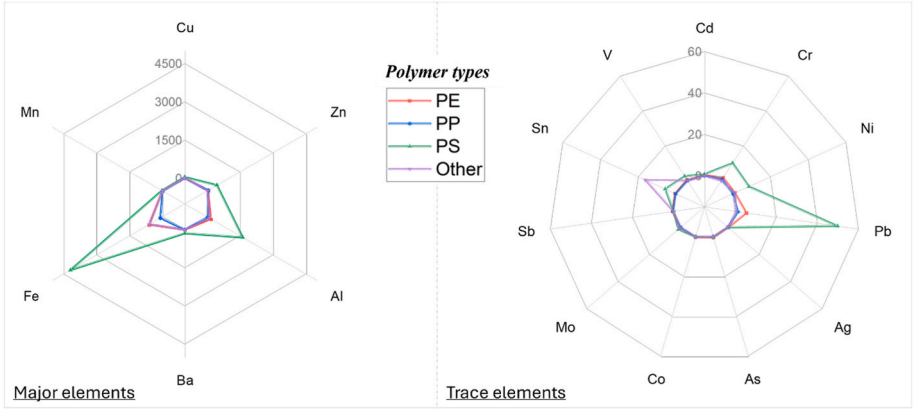

Fig. 2. – Concentration, in mg/kg, of major elements (Cu, Zn, Al, Ba, Fe, Mn) and potentially hazardous trace elements (Cd, Cr, Mn, Ni, Pb, Ag, As, Co, Hg, Mo, Sb, Sn, V) found on meso- and microplastics (PE red line, PP blue line, PS green line, Other purple line) sampled from the effluent of the investigated wastewater treatment plant. (For interpretation of the references to colour in this figure legend, the reader is referred to the Web version of this article.)

showed the highest concentrations (Fig. 2). Specifically, PS contained 10.2 ± 0.2 mg/kg of chromium, 8.6 ± 0.1 mg/kg of nickel, and 49.8 ± 0.2 mg/kg of lead, substantially exceeding the levels measured on other polymer types. Elevated concentrations of tin, vanadium, and molybdenum were also found on PS, with tin reaching 16.2 ± 0.09 mg/kg in the "Other" polymer category. Some of these inorganic elements may originate from additives in the original plastic material (Godoy et al., 2019). The elevated concentrations observed for PS may partly reflect the composition of the base material. However, as further discussed in the section on organic contaminants, increased contamination of PS is also attributable to its chemical (polymer type) and physical (shape and size) properties. Most PS particles measured between 500 and 1000 μm (Fig. 1), placing them within the MPs size range. Morphologically, they were spherical, highly degraded, and porous (Supplementary Fig. S9–S10), characteristics that substantially increase surface area and, in turn, enhance contaminant adsorption.

To evaluate the contribution of M-MPs to contaminant transport, metal(loid) concentrations on M-MPs were compared with those in SPM from the effluent (Table 1). While SPM represents the total particulate load in water, M-MPs account for only a small fraction of its mass. Polymer concentrations in effluents are generally reported between 2 and 20 μg/L (Okoffo et al., 2023; Roscher et al., 2022), compared with average SPM levels of about 20 mg/L in treated effluents (Bonomo, 2008). Despite their lower abundance, M-MPs, particularly PS, emerged as concentrated carriers of PHTEs. For instance, the average lead concentration in total SPM was 11.8 ± 0.1 mg/kg, whereas PS particles exhibited nearly fourfold higher levels, underscoring their disproportionate role in pollutant transport.

3.2.2. *Organic micropollutants*

Synthetic musk fragrances. Eight SMFs were analyzed, including Galaxolidone (HHCB-lactone), which is formed in WWTPs through the biotransformation of Galaxolide (HHCB) during biological treatment processes treatments (Tasselli and Guzzella, 2020). Fig. 3 illustrates the concentrations of SMFs and other organic micropollutants on the investigated plastic polymers, expressed in mg/kg. Numerical data corresponding to these findings are summarized in Supplementary Table S4. The most abundant compounds identified on M-MPs were HHCB-lactone, HHCB, Tonalide (AHTN), Musk xylene (MX), and Celestolide (ADBI). PS particles exhibited the highest concentrations of SMFs (e.g., ADBI: 1.2 mg/kg; HHCB: 121.5 mg/kg; HHCB-lactone: 134.9 mg/kg), with a total SMF load of 283.7 mg/kg, reflecting a strong sorption affinity for these compounds. As observed for inorganic contaminants, elevated SMF concentrations on PS can be explained by both the morphological features of PS M-MPs in effluents (Fig. 1 and Supplementary Fig. S9–S10) and the aromatic nature of PS polymer chains, which promotes interactions with aromatic molecules such as SMFs (Prajapati et al., 2022). In addition, the regular spherical morphology of most PS M-MPs suggests a primary origin, likely from intentionally manufactured products such as personal care items, which frequently contain SMFs as additives. These types of MPs fall under Commission Regulation (EU) 2023/2055 of the European Chemicals Agency, which restricts the intentional use of synthetic polymer microparticles, including non-biodegradable, insoluble plastic glitter (European Commission, 2023). While biodegradable, soluble, natural, or inorganic forms are exempt, and certain applications (such as cosmetics and detergents) benefit from transitional periods before the full ban takes effect, legacy products remain in circulation. As a result, such particles are still detected in WWTP effluents and continue to act as vectors of SMFs to the environment. PE and PP demonstrated similar adsorption trends for these chemicals, though concentrations were lower than those recorded for PS. For example, HHCB was measured at 99.6 mg/kg on PE and slightly higher at 107.7 mg/kg on PP. The category labelled "Other" polymers consistently showed significantly lower SMF concentrations. Among all analyzed media, HHCB was identified as the most prevalent SMF. Interestingly, despite regulatory restrictions and bans on MX, such as the ones implemented by the European Commission (European Commission, 2009), our findings confirm its ongoing presence in the environment, emphasizing the continued need for environmental monitoring. MX raises concerns due to its persistent, bioaccumulative nature and its known toxicity to aquatic organisms (European Commission, 2010). Its widespread detection across various environmental compartments indicates potential risks associated with long-range transport and contamination. Additionally, concentrations of ADBI (12.5 mg/kg) and HHCB-lactone (289.8 mg/kg) were notably higher in total SPM compared to M-MPs (Supplementary Table S4). Nevertheless, the overall SMF loads on SPM and M-MPs were largely comparable, reinforcing the significant affinity of plastic polymers for these low-solubility, hydrophobic micropollutants.

UV-filters. Octocrylene (OC) exhibited the highest concentrations across all media (Fig. 3), with particularly elevated levels on PS (942.4 mg/kg), followed by "Other" polymers (436.8 mg/kg), PP (97.0 mg/kg), and PE (35.3 mg/kg). 2,4-Dihydroxybenzophenone (3BP) was also enriched on PS (31.8 mg/kg). The elevated presence of OC and 3BP reflects their widespread application as UV-filtering ingredients and, given their recalcitrance in natural environments, their potential for environmental persistence and accumulation (Carvalhais et al., 2025). The strong sorption capacity of PS for UV-f can likely be attributed to effective hydrophobic and aromatic interactions. "Other" polymers carried relatively high concentrations of 3-(4-methylbenzylidene) camphor (4MBC, 6.4 mg/kg) and OC (436.8 mg/kg), suggesting a moderate to high affinity for these compounds. In PP, OC (97.0 mg/kg) and 2-ethylhexyl 4-methoxycinnamate (EHMC, 2.5 mg/kg) were most abundant, whereas other UV-f occurred at comparatively low levels. PE consistently exhibited the lowest concentrations among all polymers tested. As further discussed in Section 3, although PE and PP show lower sorption capacities for UV-f, their ubiquity in the environment makes them important contributors to contaminant transport when total polymer abundance is considered. 3-Benzylidene camphor (3BC) and 2-phenylbenzimidazole-5-sulfonic acid (OP PABA) were detected at

Table 1
– Potentially hazardous trace elements concentrations (mean values ± standard deviations, in mg/kg) found on different polymers (PE: polyethylene; PP: polypropylene; PS: polystyrene; Other: nylon-6, PE/PP copolymers, EVA, and PDM) sampled in the wastewater treatment plant effluent, and their concentration on the solid particulate matter (SPM) sampled in the same effluent. "D" indicates detection below the limit of detection (LOD), while "< LOQ" denotes concentrations between the LOD and the limit of quantification (LOQ).

Element		Cd	Cr	Cu	Ni	Pb	As	Co	Mo	Sn	V
Concentration (mg/kg)	**PE**	0.3 ± 0.003	1.7 ± 0.002	16.9 ± 0.01	1.2 ± 0.006	5.4 ± 0.01	0.4 ± 0.006	0.2 ± 0.001	0.5 ± 0.001	0.6 ± 0.001	0.4 ± 0.003
	PP	0.1 ± 0.002	0.8 ± 0.001	3.8 ± 0.03	0.2 ± 0.006	1.3 ± 0.01	< LOQ	0.03 ± 0.001	0.1 ± 0.0	0.3 ± 0.003	0.05 ± 0.0
	PS	0.7 ± 0.02	10.2 ± 0.2	46.8 ± 0.05	8.6 ± 0.1	49.8 ± 0.2	D	D	1.6 ± 0.03	5.7 ± 0.07	2.6 ± 0.02
	Other	D	D	13.2 ± 0.2	1.2 ± 0.03	0.5 ± 0.01	D	D	0.5 ± 0.01	16.2 ± 0.09	D
	SPM	1.2 ± 0.01	D	144.5 ± 0.2	32.5 ± 0.4	11.8 ± 0.1	2.2 ± 0.1	2.1 ± 0.01	7.5 ± 0.1	2.8 ± 0.03	2.4 ± 0.03

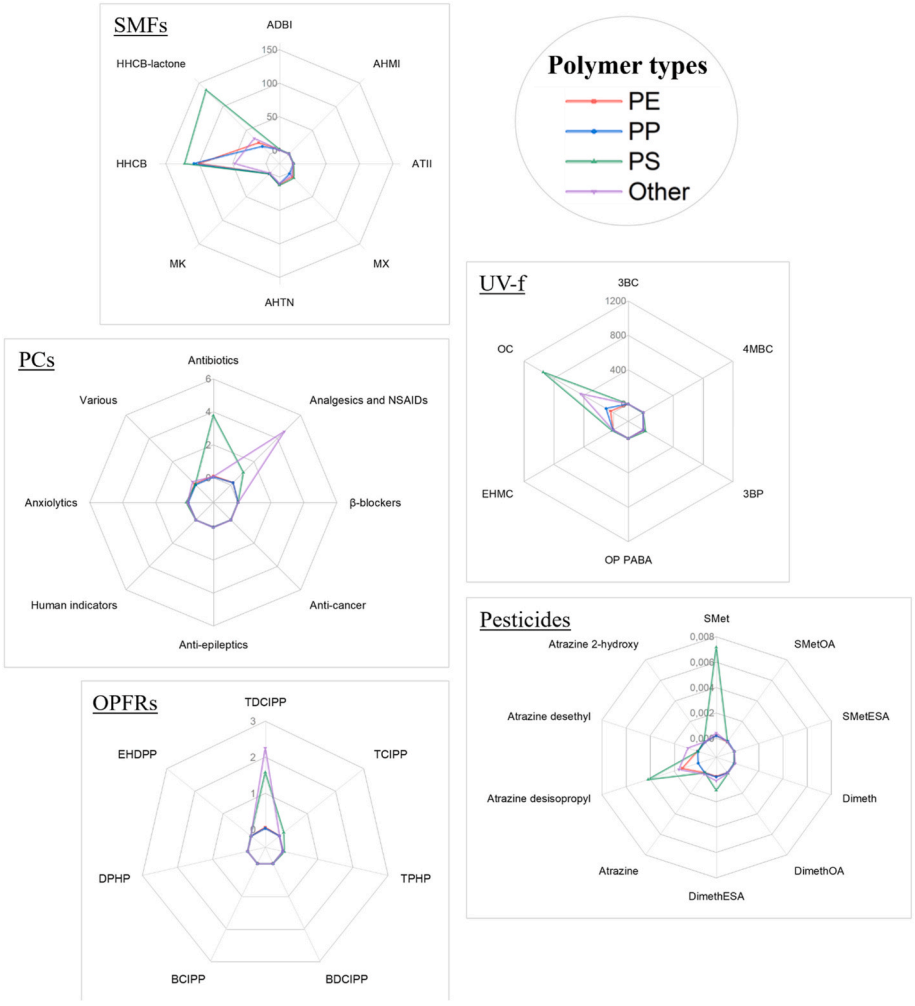

Fig. 3. Concentrations of synthetic musk fragrances (SMFs), UV-filters (UV-f), pharmaceutical compounds (PCs; grouped by pharmacological class, full list in Supplementary Table S4), organophosphate flame retardants (OPFRs), and pesticides sorbed onto different meso- and microplastic polymer types (PE, PP, PS, Other) in the wastewater treatment plant effluent. Results are expressed as mg of organic micropollutant per kg of polymer. See the List of Abbreviations (Supplementary Material) for compound definitions.

relatively low concentrations across all polymers, while 4MBC displayed high variability, with maximum values in "Other" polymers and lower levels in PS (1.0 mg/kg). In contrast, SPM accumulated lower concentrations of UV-f compared to M-MPs, with 3BP (15.2 mg/kg) and OC (38.2 mg/kg) being most abundant (Supplementary Table S4). This highlights the role of SPM as a transport medium for UV-f, though it appears less selective than plastic polymers in retaining and transporting these hydrophobic compounds.

Pharmaceuticals. Due to the wide range of PCs analyzed, they were classified by pharmacological category: antibiotics, analgesics and non-steroidal anti-inflammatory drugs (NSAIDs), β-blockers, anticancer agents, antiepileptics, anxiolytics, and miscellaneous others (Miossec et al., 2019). A complete list of the investigated compounds and their concentrations is provided in Supplementary Table S4. Fig. 3 illustrates the broad spectrum of PCs detected across all polymer types. Analgesics and NSAIDs, particularly Diclofenac, Acetaminophen (paracetamol), and Ibuprofen, were consistently detected on multiple polymers, indicating a general affinity of these compounds for M-MP surfaces. PE showed notable sorption of Acetaminophen and the diuretic Hydrochlorothiazide (both 0.1 mg/kg), along with detectable levels of the fluoroquinolone antibiotics Norfloxacin and Ofloxacin. By contrast, Ibuprofen, Amoxicillin, and Sulfadiazine were not detected on PE. PP exhibited overall lower retention of PCs than PE, with only low levels of Ibuprofen (0.03 mg/kg) and Acetaminophen (0.1 mg/kg), and minimal antibiotic adsorption. In contrast, PS demonstrated the highest sorption capacity for many compounds. Significant concentrations were observed for the NSAID Acide Niflumique (0.3 mg/kg), Diclofenac (0.5 mg/kg), and Ofloxacin (0.5 mg/kg). Notably, PS also exhibited substantial adsorption of the macrolide antibiotic Azithromycin (3.2 mg/kg), likely reflecting strong hydrophobic interactions (Log K_{ow} = 4) and polymer-specific surface affinity mechanisms. The "Other" polymer category displayed a distinct adsorption profile, dominated by analgesics and NSAIDs. Ibuprofen reached its highest concentration in this group (3.7 mg/kg), accompanied by Diclofenac (0.5 mg/kg) and Acide Niflumique (0.3 mg/kg). Spiramycin, another macrolide antibiotic, was also detected (0.05 mg/kg), further distinguishing this group from the other polymer types. SPM exiting the WWTP accumulated higher total concentrations of PCs than M-MPs, underscoring its role as a major sink for compounds escaping removal during treatment. Azithromycin (47.4 mg/kg) and Spiramycin (32.4 mg/kg) were dominant, followed by Ibuprofen (6.9 mg/kg) and the β-blocker Atenolol (4.7 mg/kg). These findings emphasize the significant role of SPM in the environmental transport and fate of PCs, with potential implications for both aquatic and benthic ecosystems. Such considerations should be incorporated into comprehensive strategies to control PC emissions from wastewater, particularly in light of Directive (EU) 2024/3019 on urban wastewater treatment, which establishes benchmark removal requirements for selected pharmaceuticals during treatment processes. Interestingly,

traces of anticancer, antiepileptic, and anxiolytic compounds were detected exclusively on M-MPs and not on SPM, as detailed in Supplementary Table S4.

OPFRs. PE and PP exhibit lower adsorption levels compared to PS, which consistently showed high adsorption of multiple OPFRs (Fig. 3), particularly tris(1,3-dichloro-2-propyl) phosphate (TDCIPP) and triphenyl phosphate (TPHP). This pronounced adsorption by PS could be attributed to its hydrophobicity and potential π-π interactions with aromatic OPFRs like TPHP (Martín et al., 2022). The "Other" category displayed intermediate adsorption levels. Among the OPFRs, TDCIPP demonstrated the highest adsorption across all polymers (Fig. 3), with the most significant levels observed on "Other" (2.2 mg/kg) and PS (1.6 mg/kg). TPHP was predominantly adsorbed on PS (0.04 mg/kg), while PE and PP showed much lower adsorption levels. Low levels of bis(1, 3-dichloro-2-propyl) phosphate (BCIPP) and diphenyl phosphate (DPHP), both OPFRs metabolites, were detected only on PP (Supplementary Table S4). The adsorption of 2-ethylhexyl diphenyl phosphate (EHDPP) was relatively low across all polymers but showed slightly higher concentrations on PS. The overall SPM exhibited the highest adsorption levels for several OPFRs, particularly TCIPP (4.6 mg/kg), and TPHP (0.8 mg/kg), highlighting its critical role in the environmental distribution of these compounds. However, bis(1, 3-dichloro-2-propyl) phosphate (BDCIPP), BCIPP, and DPHP could not be measured on the SPM, while they could on PP and PE M-MPs (Supplementary Table S4).

Pesticides. The pesticide concentration found on M-MPs were lower compared to the other micropollutants investigated (Fig. 3). PS demonstrates significantly higher adsorption levels for several pesticides, especially S-Metolachlor (0.007 mg/kg) and Atrazine desisopropyl (0.004 mg/kg). Additionally, as reported in Supplementary Table S4, PS showed measurable adsorption of Dimethenamid ESA and Atrazine 2-hydroxy, suggesting its capacity to adsorb diverse pesticide compounds. In contrast, PE and PP exhibit lower adsorption levels, reflecting limited interactions with most pesticides. PE primarily adsorbed Atrazine desisopropyl and Atrazine desethyl, while PP showed minimal adsorption of S-Metolachlor and Atrazine desethyl. Both polymers exhibit negligible adsorption for the other pesticides. "Other" polymers demonstrate moderate adsorption levels for Atrazine desisopropyl (0.002 mg/kg) and Atrazine desethyl (0.001 mg/kg). As expected, SPM exhibits the highest adsorption levels overall, particularly for S-Metolachlor (0.1 mg/kg). However, SPM showed negligible adsorption for many other compounds. PS and SPM emerge as key actors for pesticide adsorption, with PS showing strong interactions for aromatic pesticides and SPM serving as a central repository for specific molecules. PE, PP, and "Other" polymers demonstrate relatively low pesticide adsorption, with occasional exceptions based on pesticide type. These results are reasonable, since pesticide concentrations in the raw wastewater (influent, data not reported) sample were low. Furthermore, pesticides are generally highly hydrophilic, more prone to be present in dissolved form (Barbieri et al., 2019).

In the Supplementary Table S6, we report the Log K_{ow} (NIH - PubChem, XLogP3-AA computational method) for most of investigated organic micropollutants. SMFs, UV-f, and OPFRs exhibit the highest Log K_{ow} values among organic micropollutants, indicative of strong hydrophobicity, generally linked to low solubility. This characteristic implies a preference for these compounds to partition into non-polar environments, such as non-polar areas of M-MPs surfaces. Conversely, compounds with low Log K_{ow} values, such as PCs and pesticides, are more hydrophilic and demonstrate greater solubility in water. These trends are consistent with our findings, where hydrophobic contaminants were present in significantly higher concentrations on M-MPs compared to their hydrophilic counterparts (Fig. 3). This indicates that the interaction between contaminants and M-MPs is influenced, among other factors, by the hydrophobicity or hydrophilicity of the compounds, as indicated by Log K_{ow}.

3.3. Micropollutant emissions into the environment

Daily micropollutant fluxes (mg day^{-1}) were calculated across the main plant streams (dissolved fraction, SPM-bound fraction in influent and effluent, M-MPs, and dewatered sludge) using the average influent and effluent flow rates together with sludge output data provided by the plant operator. Full numerical values are reported in Supplementary Table S5, while Fig. 4 illustrates the distribution of micropollutant loads among the different M-MP polymer types.

Polymer-dependent micropollutant transport. PE emerged as the dominant polymer vector, contributing nearly 80 % of the elemental fluxes and the majority of organic micropollutants associated with M-MPs. PP also played an important role, particularly in transporting UV-f and PCs. The distribution of SMFs was relatively balanced, with approximately 60 % sorbed to PE and 40 % to PP (Fig. 4d).

Emissions of inorganic micropollutants. M-MPs transported measurable amounts of several elements, including 249 mg day^{-1} of iron, 75 mg day^{-1} of aluminium, 32 mg day^{-1} of zinc, and 7 mg day^{-1} of copper. Smaller fluxes of lead (2.2 mg day^{-1}), chromium (0.8 mg day^{-1}), nickel (0.5 mg day^{-1}), tin (0.4 mg day^{-1}), and cadmium (0.1 mg day^{-1}) were also detected. However, these values were negligible compared to the total effluent fluxes, which reached 1.3 kg day^{-1} for iron, 0.8 kg day^{-1} for zinc, 0.4 kg day^{-1} for aluminium, and 0.7 kg day^{-1} for manganese, alongside notable emissions of copper (79 g day^{-1}), nickel and molybdenum (23 g day^{-1} each), lead (17 g day^{-1}), arsenic (15 g day^{-1}), vanadium (11 g day^{-1}), antimony (10 g day^{-1}), and chromium (8 g day^{-1}). These dissolved concentrations are consistent with previously reported ranges for urban wastewaters (Kinuthia et al., 2020). Dewatered sludge acted as the primary sink, retaining approximately 12 kg day^{-1} of iron, 18 kg day^{-1} of aluminium, 1.6 kg day^{-1} of zinc, 125 g day^{-1} of lead, 35 g day^{-1} of chromium, and 0.7 g day^{-1} of mercury.

Emissions of organic micropollutants. Among organic contaminants, the six most abundant compounds sorbed to M-MPs were HHCB (55.6 mg day^{-1}), OC (38.8 mg day^{-1}), HHCB-lactone (11.8 mg day^{-1}), AHTN (5.9 mg day^{-1}), MX (3.1 mg day^{-1}), and 3BP (2.8 mg day^{-1}). Nonetheless, SPM transported much higher overall loads. For example, SMFs accounted for ~192 g day^{-1} in total emissions, of which SPM carried ~70 g day^{-1} compared to only 78.5 mg day^{-1} on M-MPs. A similar pattern was observed for UV-f, with 25.5 g day^{-1} associated with SPM and 42.8 mg day^{-1} with M-MPs. PCs were largely present in dissolved form, with 26.6 g day^{-1} transported by SPM and just 0.3 mg day^{-1} by M-MPs. OPFRs also showed limited association with plastics, with M-MPs carrying ~55 μg day^{-1} (mainly TDCIPP and TCIPP) compared to 3.7 g day^{-1} in the effluent, of which 1.4 g day^{-1} was SPM-bound. Pesticides displayed the weakest association with M-MPs (0.7 μg day^{-1}), with atrazine desisopropyl and S-metolachlor being the main representatives. The latter also dominated in SPM, accounting for most of the pesticide flux.

In general, hydrophobic micropollutants such as SMFs and UV-f were more efficiently retained in sludge, with estimated daily removals of 401 g and 610 g, respectively (Supplementary Table S5). Conversely, more hydrophilic compounds such as PCs, OPFRs, and pesticides exhibited limited sludge affinity and were predominantly discharged with the effluent. For example, pesticides were released at a rate of 283 mg day^{-1}, while only 18 mg day^{-1} were sequestered in dewatered sludge.

4. Discussion

Although the overall micropollutant fluxes transported by M-MPs were lower than those carried by the dissolved phase or bulk suspended solids, M-MPs represent discrete, mobile niches with the capacity to concentrate and mobilize specific contaminants beyond conventional treatment barriers (De Souza et al., 2025). The detection of atrazine desisopropyl on M-MPs, but not on SPM, points to selective adsorption mechanisms and divergent partitioning behavior. This agrees with

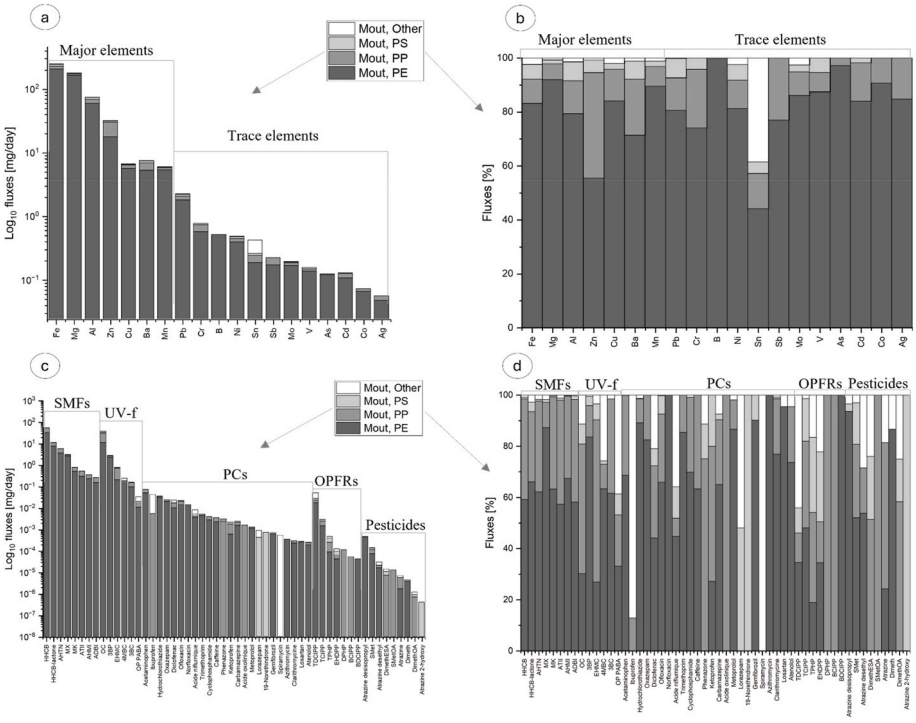

Fig. 4. Total net fluxes (mg/day) of the investigated inorganic and organic contaminants, presented on a Log_{10} scale, are shown in Fig. 4a and c. The percentage contributions of different polymers to the total flux of each contaminant are illustrated in Fig. 4b and d. M_{out}, X represents the total mass of a contaminant leaving the wastewater treatment plant *via* polymer X (X = PE, PP, PS, Other). SMFs: synthetic musk fragrances; UV-f: UV-filters; PCs: pharmaceutical compounds; OPFRs: organophosphate flame retardants.

previous studies showing that aged MPs exhibit higher sorption capacities for pesticides such as atrazine compared to pristine particles (Y. Wang et al., 2022). Such observations underscore the importance of considering M-MPs not only as passive carriers but as dynamic vectors capable of altering contaminant partitioning and persistence in effluents.

Hydrophobic and organophilic compounds, such as SMFs and UV-f, were particularly enriched on M-MPs despite their high removal rates *via* sludge retention. Their persistence on plastics in the final effluent highlights an overlooked emission pathway. Polymer-specific differences further modulate sorption. The predominance of PE as a contaminant vector appears linked to its abundance in wastewater (Ren et al., 2020) rather than a superior intrinsic affinity. PP showed notable associations with UV-f and PCs, while PS, though less abundant, displayed the highest mass-specific sorption. This likely reflects surface weathering and the development of reactive groups such as hydroxyl, carboxyl, and amino functionalities, which enhance interactions with polar molecules (Prajapati et al., 2022). Additional particle properties, including small size, high surface-area-to-volume ratio, porosity, and surface roughness, further increase sorption potential (Agboola and Benson, 2021). It should be noted that specific surface area was not measured in this study, and differences between M-MPs and bulk SPM may influence sorption capacities; hence, direct comparisons should be interpreted with caution. It should also be noted that our extraction methods target the fraction of contaminants readily available at or near the plastic surface; pollutants that have diffused deeper into aged polymers may not be fully recovered, but this fraction is most relevant for environmental exposure and sorption processes.

Measured metal concentrations on M-MPs may reflect both contaminants adsorbed from wastewater and inorganic additives or residual catalysts inherent to the polymer matrix; thus, enrichment patterns should be interpreted considering both sources. Interestingly, the category of "Other" polymers, although minor in abundance, accounted for disproportionate fluxes of certain pollutants such as tin and OPFRs, highlighting the need for comprehensive polymer characterisation beyond dominant resin types. The high sorption observed for these minor polymers may reflect distinct chemical interactions related to surface functional groups, polymer aging, or additives, which warrants further investigation in future studies.

Future research should therefore expand toward a broader range of polymer types and smaller size classes, down to the nanoscale, to fully capture the contribution of plastic particles to micropollutant transport and exposure risks. At the same time, methodological challenges must be addressed by balancing reliable polymer identification with the preservation of sorbed contaminants and the so-called ecocorona, a complex biological and chemical interface known to regulate adsorption, transport, and degradation processes (Shi et al., 2023). Humic substances represent key constituents of the ecocorona and strongly influence surface charge and sorption behavior. Recent studies have shown that advanced treatment processes, such as electrocoagulation, can effectively remove humic acids from wastewater (Asgharian et al., 2017), suggesting that upstream removal of ecocorona precursors may indirectly modify MPs surface chemistry and reduce their potential role as contaminant vectors. The presence of a biofilm or ecocorona on environmentally aged MPs may influence the reported mass-normalized micropollutant concentrations in two opposing ways. Biofilm development adds organic and inorganic material to the particle mass, which may slightly dilute concentrations when normalized per unit mass of the MPs–ecocorona complex. Conversely, biofilms substantially increase the availability of sorption sites through extracellular polymeric substances, microbial biomass, and associated OM, thereby enhancing affinity for metals and organic contaminants. Biofilm thickness and composition are known to vary with polymer type, exposure time, and environmental conditions, and biofilm-coated MPs have been shown to accumulate higher contaminant loads than pristine particles despite their limited mass contribution (Rummel et al., 2017; Richard et al., 2019). Biofilms can promote the accumulation of trace metals and organic pollutants by providing additional binding phases and redox-active

microenvironments (Richard et al., 2019). Accordingly, the mass-based concentrations reported here reflect the combined contribution of the polymer core and its associated biofilm and should be interpreted as representative of environmentally realistic MPs complexes rather than pristine materials. This integrated perspective is consistent with current evidence highlighting the functional importance of the ecocorona in governing contaminant transport and biological interactions, even when its contribution to total particle mass remains comparatively small (Rummel et al., 2017).

Several methodological constraints of this study likely led to conservative flux estimates. Only particles with unambiguous FTIR spectra were retained, and no chemical purification was applied to avoid desorption of micropollutants. Consequently, some visually suspected plastics were excluded. Moreover, the analysis was restricted to particles larger than 300 μm, excluding the 1–300 μm fraction that may carry a significant share of the contaminant load (Joo et al., 2021). This size class is of particular concern because MPs in the 1–100 μm range are likely the most abundant and can physically damage mucosal tissues, obstruct feeding structures, and impair locomotion in aquatic biota (Casagrande et al., 2024). Even smaller nanoplastics pose greater ecotoxicological risks due to their ability to penetrate biological membranes, reach subcellular compartments, and induce oxidative stress, inflammation, and genotoxicity (Bakan et al., 2024). These considerations reinforce the importance of size-inclusive monitoring strategies and holistic assessments of plastic-associated contaminant fluxes.

The predominance of pharmaceutical residues in the dissolved phase highlights the limited removal efficiency of conventional treatment processes and reinforces the need for advanced tertiary or quaternary treatment stages. These include established technologies such as ozonation and activated carbon filtration, applied alone or in combination (Bernabeu et al., 2011), as well as emerging hybrid approaches such as simultaneous electrocoagulation–electrooxidation, which have been shown to effectively degrade recalcitrant antibiotics including cephalosporins (Danaee et al., 2025). These findings align with recent policy developments, notably Directive (EU) 2024/3019, which sets new benchmarks for micropollutant removal in urban wastewater treatment. A key challenge lies in implementing treatment solutions that are both broad-spectrum and environmentally sustainable, given the chemical diversity and variable behavior of wastewater contaminants. In this context, prevention remains a critical complementary strategy, as reducing emissions at source and promoting the use of biodegradable and less hazardous substances can substantially limit downstream environmental burdens and associated risks. Beyond effluent discharge, the reuse of sewage sludge in agriculture raises additional concerns. Micropollutants tend to accumulate in biosolids, particularly on high-affinity solid phases, and their co-occurrence may amplify environmental and human health risks (Fytili and Zabaniotou, 2008). The detection of organically bound mercury in dewatered sludge in this study further underscores the need for site-specific toxicity and ecological risk assessments, including the evaluation of potential transformation products and combined effects, as highlighted by recent methodological approaches (Nateq et al., 2024), prior to land application.

5. Conclusions

This study demonstrates that meso- and microplastics (M-MPs) serve as effective vectors for both organic and inorganic micropollutants, including potentially hazardous trace elements, synthetic musk fragrances, UV filters, pharmaceuticals, organophosphate flame retardants, and pesticides. Even a few milligrams of plastic were sufficient to carry measurable loads of virtually all targeted compounds, underscoring the disproportionate role of M-MPs in contaminant mobility. Their heterogeneous and weathered surfaces, enriched with copolymers, additives, and oxidation products, provide diverse sorption sites for molecules of varying polarity. In natural environments, the acquisition of an ecocorona further enhances their capacity to capture micropollutants and increases their bioaccessibility, highlighting M-MPs as mobile hotspots for pollutant transport.

Among the polymers analyzed, aged polystyrene fragments emerged as particularly efficient vectors due to their surface chemistry and morphology, although polyethylene and polypropylene contributed most to total fluxes because of their higher abundance. While this study focused on particles >300 μm, smaller microplastics and nanoplastics, owing to their higher surface-area-to-mass ratios and greater reactivity, are expected to play an even more critical role in contaminant transport. The fluxes reported here therefore represent conservative estimates of plastic-associated emissions from WWTPs. Future research should encompass the full-size spectrum of plastic particles, ideally down to the nanoscale, to provide a more comprehensive understanding of their contribution to contaminant transfer within complex particulate matrices. Such work should also investigate how particle morphology (e.g., shape, porosity, surface roughness) and the formation of the ecocorona influence adsorption dynamics under real-world conditions. This will be essential for improving risk assessments and developing effective management strategies aimed at limiting the environmental persistence, mobility, and ecological impacts of micropollutants discharged from wastewater treatment plants.

CRediT authorship contribution statement

Simone Cavazzoli: Writing – original draft, Visualization, Software, Methodology, Investigation, Formal analysis, Data curation, Conceptualization. **Marie Morere:** Writing – review & editing, Formal analysis. **Gianni Andreottola:** Writing – review & editing, Supervision, Funding acquisition, Data curation, Conceptualization. **Mathilde Monperrus:** Writing – review & editing, Supervision, Resources, Methodology, Investigation, Funding acquisition, Formal analysis, Data curation.

Declaration of generative AI and AI-assisted technologies in the writing process

During the preparation of this work the author(s) used ChatGPT to improve the language and readability of the manuscript. After using this tool/service, the author(s) reviewed and edited the content as needed and take(s) full responsibility for the content of the publication.

Funding sources

This research did not receive any specific grant from funding agencies in the public, commercial, or not-for-profit sectors.

Declaration of competing interest

The authors declare that they have no known competing financial interests or personal relationships that could have appeared to influence the work reported in this paper.

Acknowledgements

We acknowledge E. Germain for his invaluable support during experimental activities, and R. Larrède and D. Lafargue for their help at the WWTP. We also acknowledge the Italian Ministry of Universities and Research for funding S.C.'s PhD scholarship (37th Cycle PhD Programmes supported by ESF REACT-EU funds, National Operational Programme on Research and Innovation).

Appendix A. Supplementary data

Supplementary data to this article can be found online at https://doi.org/10.1016/j.envres.2026.123825.

References

Acarer, S., 2023. Microplastics in wastewater treatment plants: sources, properties, removal efficiency, removal mechanisms, and interactions with pollutants. Water Sci. Technol. 87 (3), 685–710. https://doi.org/10.2166/wst.2023.022.

Agboola, O.D., Benson, N.U., 2021. Physisorption and chemisorption mechanisms influencing Micro (Nano) plastics-organic chemical contaminants interactions: a review. Front. Environ. Sci. 9. https://www.frontiersin.org/articles/10.3389/fenvs.2021.678574.

Ali, I., Ding, T., Peng, C., Naz, I., Sun, H., Li, J., Liu, J., 2021. Micro- and nanoplastics in wastewater treatment plants: occurrence, removal, fate, impacts and remediation technologies – a critical review. Chem. Eng. J. 423. https://doi.org/10.1016/j.cej.2021.130205.

Al-Mamun, M.R., Kader, S., Islam, M.S., Khan, M.Z.H., 2019. Photocatalytic activity improvement and application of UV-TiO2 photocatalysis in textile wastewater treatment: a review. J. Environ. Chem. Eng. 7 (5). https://doi.org/10.1016/j.jece.2019.103248.

Amaral-Zettler, L.A., Zettler, E.R., Mincer, T.J., 2020. Ecology of the plastisphere. Nat. Rev. Microbiol. 18 (3), 139–151. https://doi.org/10.1038/s41579-019-0308-0.

Asgharian, F., Khosravi-Nikou, M.R., Anvaripour, B., Danaee, I., 2017. Electrocoagulation and ultrasonic removal of humic acid from wastewater. Environ. Prog. Sustain. Energy 36 (3), 822–829. https://doi.org/10.1002/ep.12512.

Bakan, B., Kalčec, N., Liu, S., Ilić, K., Qi, Y., Capjak, I., Božičević, L., Peranić, N., Vrček, I. V., 2024. Science-based evidence on pathways and effects of human exposure to micro- and nanoplastics. Arh. Hig. Rada. Toksikol. 75 (1), 1–14. https://doi.org/10.2478/aiht-2024-75-3807.

Barbieri, M.V., Postigo, C., Monllor-Alcaraz, S., Barcelo, D., Alda, M. L. de, 2019. Reliable LC-MS/MS-based method for trace level determination of 50 medium to highly polar pesticide residues in sediments and ecological risk assessment. Anal. Bioanal. Chem. 411 (30), 7981–7996. https://doi.org/10.1007/s00216-019-02188-0.

Bernabeu, A., Vercher, R.F., Santos-Juanes, L., Simón, P.J., Lardín, C., Martínez, M.A., Vicente, J.A., González, R., Llosá, C., Arques, A., Amat, A.M., 2011. Solar photocatalysis as a tertiary treatment to remove emerging pollutants from wastewater treatment plant effluents. Catal. Today 161 (1), 235–240. https://doi.org/10.1016/j.cattod.2010.09.025.

Bexfield, L.M., Toccalino, P.L., Belitz, K., Foreman, W.T., Furlong, E.T., 2019. Hormones and pharmaceuticals in groundwater used as a source of drinking water across the United States. Environ. Sci. Technol. 53 (6), 2950–2960. https://doi.org/10.1021/acs.est.8b05592.

Blum, A., Behl, M., Birnbaum, L.S., Diamond, M.L., Phillips, A., Singla, V., Sipes, N.S., Stapleton, H.M., Venier, M., 2019. Organophosphate Ester flame retardants: are they a regrettable substitution for polybrominated diphenyl ethers? Environ. Sci. Technol. Lett. 6 (11), 638–649. https://doi.org/10.1021/acs.estlett.9b00582.

Bonomo, L., 2008. Trattamenti Delle Acque Reflue. McGraw-Hill Companies.

Cao, S., Duan, X., Zhao, X., Ma, J., Dong, T., Huang, N., Sun, C., He, B., Wei, F., 2014. Health risks from the exposure of children to As, Se, Pb and other heavy metals near the largest coking plant in China. Sci. Total Environ. 472, 1001–1009. https://doi.org/10.1016/j.scitotenv.2013.11.124.

Carvalhais, A., Lippa, R., Oliveira, I.B., Di Lorenzo, G., Mieiro, C., Pacheco, M., 2025. Effects of the UV filter octocrylene and its degradation product benzophenone on Pacific Oyster (Magallana gigas) larvae: a call for reassessment of environmental hazards. Toxics 13 (3), 177. https://doi.org/10.3390/toxics13030177.

Casagrande, N., Verones, F., Sobral, P., Martinho, G., 2024. Physical properties of microplastics affecting the aquatic biota: a review. Environ. Adv. 17, 100566. https://doi.org/10.1016/j.envadv.2024.100566.

Cavalheiro, J., Zuloaga, O., Prieto, A., Preudhomme, H., Amouroux, D., Monperrus, M., 2017. Occurrence and fate of organic and organometallic pollutants in municipal wastewater treatment plants and their impact on receiving waters (Adour estuary, France). Arch. Environ. Contamin. Toxicol. 73, 137–152. https://doi.org/10.1007/s00244-017-0422-9.

Cavazzoli, S., Ferrentino, R., Scopetani, C., Monperrus, M., Andreottola, G., 2023. Analysis of micro- and nanoplastics in wastewater treatment plants: key steps and environmental risk considerations. Environ. Monit. Assess. 195 (12), 1483. https://doi.org/10.1007/s10661-023-12030-x.

Cavazzoli, S., Murari, F., Donegà, M., Tirler, W., Andreottola, G., 2025a. Microplastic removal and environmental emissions from municipal wastewater treatment plants. J. Clean. Prod. 521, 146267. https://doi.org/10.1016/j.jclepro.2025.146267.

Cavazzoli, S., Scopetani, C., Chelazzi, D., Martellini, T., Cincinelli, A., Carretti, E., Ascolese, M., Gori, R., Mair, K., Tirler, W., Donegà, M., Andreottola, G., 2025b. Effectiveness of conventional municipal wastewater treatment plants in microplastics removal: insights from multiple analytical techniques. J. Environ. Sci. https://doi.org/10.1016/j.jes.2025.04.035. S1001074225002098.

Danaee, I., Ghanbari, F., Mohseni-Bandpei, A., Rashidi, M., 2025. Enhanced cephalosporin antibiotics degradation through simultaneous electrocoagulation–electrooxidation. J. Water Process Eng. 51, 108878. https://doi.org/10.1016/j.jwpe.2025.108878.

De Souza, L.G.X., Teran, F.J.C., Cuba, R.M.F., Chaves, A.R., Da Silva, K.C., 2025. Interaction of microplastics with emerging organic pollutants: a study on atrazine adsorption and phytotoxicity. Toxics 13 (4), 257. https://doi.org/10.3390/toxics13040257.

Debroy, A., George, N., Mukherjee, G., 2022. Role of biofilms in the degradation of microplastics in aquatic environments. J. Chem. Technol. Biotechnol. 97 (12), 3271–3282. https://doi.org/10.1002/jctb.6978.

Dong, Y., et al., 2020. Adsorption of arsenite to polystyrene microplastics in the presence of humus (humic and fulvic acids). Environ. Sci. Process. Impacts 22 (4), 781–791. https://doi.org/10.1039/d0em00324g.

Elseblani, R., Cobo-Golpe, M., Godin, S., Jimenez-Lamana, J., Fakhri, M., Rodríguez, I., Szpunar, J., 2023. Study of metal and organic contaminants transported by microplastics in the Lebanese coastal environment using ICP-MS, GC-MS, and LC-MS. Sci. Total Environ. 887, 164111. https://doi.org/10.1016/j.scitotenv.2023.164111.

EU, 2024. Directive (EU) 2024/3019 of the European Parliament and of the Council of 27 November 2024 Concerning Urban Wastewater Treatment (recast) (Text with EEA relevance).

European Commission, 2009. Commission Regulation (EC) No 552/2009 of 22 June 2009 Amending Regulation (EC) No 1907/2006 of the European Parliament and of the Council on the Registration, Evaluation, Authorisation and Restriction of Chemicals (REACH) as Regards Annex Xviitext with EEA Relevance.

European Commission, 2010. European Union Risk Assessment Report: 5-Tert-Butyl-2,4,6-Trinitro-M-Xylene (Musk Xylene). Publications Office. https://data.europa.eu/doi/10.2788/45153.

European Commission, 2023. Commission Regulation (EU) 2023/2055 of 25 September 2023 amending Annex XVII to Regulation (EC) No 1907/2006 (REACH) as regards synthetic polymer microparticles (the microplastics restriction). Official J. Eur. Union, L 277, 11–41.

Fu, L., Li, J., Wang, G., Luan, Y., Dai, W., 2021. Adsorption behavior of organic pollutants on microplastics. Ecotoxicol. Environ. Saf. 217. https://doi.org/10.1016/j.ecoenv.2021.112207.

Fytili, D., Zabaniotou, A., 2008. Utilization of sewage sludge in EU application of old and new methods—A review. Renew. Sustain. Energy Rev. 12 (1), 116–140. https://doi.org/10.1016/j.rser.2006.05.014.

Galloway, T.S., Cole, M., Lewis, C., 2017. Interactions of microplastic debris throughout the marine ecosystem. Nat. Ecol. Evol. 1, 116. https://doi.org/10.1038/s41559-017-0116.

Gavlová, A., Jachimowicz, P., Praus, P., Bednár, P., 2025. Environment changes everything: how relevant are laboratory studies of sorption of pollutants on microplastics? A critical review. J. Environ. Chem. Eng. 13 (2), 115655. https://doi.org/10.1016/j.jece.2025.115655.

Godoy, V., Blázquez, G., Calero, M., Quesada, L., Martín-Lara, M.A., 2019. The potential of microplastics as carriers of metals. Environ. Pollut. 255. https://doi.org/10.1016/j.envpol.2019.113363.

Iordachescu, L., Papacharalampos, K., Barritaud, L., Denieul, M.-P., Plessis, E., Baratto, G., Julien, V., Vollertsen, J., 2024. Microplastics in an advanced wastewater treatment plant: sustained and robust removal rates unfazed by seasonal variations. Microplastics and Nanoplastics 4 (1). https://doi.org/10.1186/s43591-024-00097-3.

Joo, S.H., Liang, Y., Kim, M., Byun, J., Choi, H., 2021. Microplastics with adsorbed contaminants: mechanisms and treatment. Environ. Chall. 3, 100042. https://doi.org/10.1016/j.envc.2021.100042.

Jung, M.R., Horgen, F.D., Orski, S.V., Rodriguez, C.V., Beers, K.L., Balazs, G.H., Jones, T. T., Work, T.M., Brignac, K.C., Royer, S.-J., Hyrenbach, K.D., Jensen, B.A., Lynch, J. M., 2018. Validation of ATR FT-IR to identify polymers of plastic marine debris, including those ingested by marine organisms. Mar. Pollut. Bull. 127, 704–716. https://doi.org/10.1016/j.marpolbul.2017.12.061.

Kinuthia, G.K., Ngure, V., Beti, D., Lugalia, R., Wangila, A., Kamau, L., 2020. Levels of heavy metals in wastewater and soil samples from open drainage channels in Nairobi, Kenya: community health implication. Sci. Rep. 10 (1), 8434. https://doi.org/10.1038/s41598-020-65359-5.

Kopatz, V., Wen, K., Kovács, T., Keimowitz, A.S., Pichler, V., Widder, J., Vethaak, A.D., Hollóczki, O., Kenner, L., 2023. Micro- and nanoplastics breach the blood–brain barrier (BBB): biomolecular corona's role revealed. Nanomaterials 13 (8). https://doi.org/10.3390/nano13081404. Article 8.

Kumar, M., Chen, H., Sarsaiya, S., Qin, S., Liu, H., Awasthi, M.K., Kumar, S., Singh, L., Zhang, Z., Bolan, N.S., Pandey, A., Varjani, S., Taherzadeh, M.J., 2021. Current research trends on micro- and nano-plastics as an emerging threat to global environment: a review. J. Hazard Mater. 409. https://doi.org/10.1016/j.jhazmat.2020.124967.

Li, W., Nanaboina, V., Chen, F., Korshin, G.V., 2016. Removal of polycyclic synthetic musks and antineoplastic drugs in ozonated wastewater: quantitation based on the data of differential spectroscopy. J. Hazard Mater. 304, 242–250. https://doi.org/10.1016/j.jhazmat.2015.10.035.

Mackay, D., Clark, K.E., 1991. Predicting the environmental partitioning of organic contaminants and their transfer to biota. In: Jones, K.C. (Ed.), Organic Contaminants in the Environment, Environmental Management Series, 19. Springer, Dordrecht, pp. 159–188. https://doi.org/10.1007/978-94-009-4329-2_5.

Markley, L., Driscoll, C., Hartnett, B., Mark, N., Cárdenas, A., Hapich, H., 2024. Guide for the visual identification and classification of plastic particles. https://doi.org/10.13140/RG.2.2.27505.45927.

Martín, J., Santos, J.L., Aparicio, I., Alonso, E., 2022. Microplastics and associated emerging contaminants in the environment: analysis, sorption mechanisms and effects of co-exposure. Trends in Environmental Analytical Chemistry 35, e00170. https://doi.org/10.1016/j.teac.2022.e00170.

Miossec, C., Lanceleur, L., Monperrus, M., 2019. Multi-residue analysis of 44 pharmaceutical compounds in environmental water samples by solid-phase extraction coupled to liquid chromatography-tandem mass spectrometry. J. Separ. Sci. 42 (10), 1853–1866. https://doi.org/10.1002/jssc.201801214.

Nateq, K., Amarzadeh, M., Shohani Zadeh, M., Rostami, M., Danaee, I., Schwaminger, S., Khosravi-Nikou, M.R., Mirzapoor, A., Gol, G., 2024. Ecological hazard assessment and toxicity alleviation. J. Water Process Eng. 68, 106361. https://doi.org/10.1016/j.jwpe.2024.106361.

Nguyen, B., Claveau-Mallet, D., Hernandez, L.M., Xu, E.G., Farner, J.M., Tufenkji, N., 2019. Separation and analysis of microplastics and nanoplastics in complex

environmental samples. Acc. Chem. Res. 52 (4), 858–866. https://doi.org/10.1021/acs.accounts.8b00602.
Niari, M.H., Jaafarzadeh, N., Dobaradaran, S., Niri, M.V., Dargahi, A., 2023. Release of microplastics to the environment through wastewater treatment plants: study on four types of wastewater treatment processes. Water, Air, Soil Pollut. 234 (9), 589. https://doi.org/10.1007/s11270-023-06594-0.
Okoffo, E.D., Rauert, C., Thomas, K.V., 2023. Mass quantification of microplastic at wastewater treatment plants by pyrolysis-gas chromatography–mass spectrometry. Sci. Total Environ. 856, 159251. https://doi.org/10.1016/j.scitotenv.2022.159251.
Osman, A.I., Hosny, M., Eltaweil, A.S., Omar, S., Elgarahy, A.M., Farghali, M., Yap, P.-S., Wu, Y.-S., Nagandran, S., Batumalaie, K., Gopinath, S.C.B., John, O.D., Sekar, M., Saikia, T., Karunanithi, P., Hatta, M.H.M., Akinyede, K.A., 2023. Microplastic sources, formation, toxicity and remediation: a review. Environ. Chem. Lett. 21 (4), 2129–2169. https://doi.org/10.1007/s10311-023-01593-3.
Pagliaccia, B., Ascolese, M., Vannini, E., Carretti, E., Lubello, C., Gori, R., 2025. Methodologic insights aimed to set-up an innovative laser direct InfraRed (LDIR)-based method for the detection and characterization of microplastics in wastewaters. Sci. Total Environ. 967, 178817. https://doi.org/10.1016/j.scitotenv.2025.178817.
Parida, V.K., Saidulu, D., Majumder, A., Srivastava, A., Gupta, B., Gupta, A.K., 2021. Emerging contaminants in wastewater: a critical review on occurrence, existing legislations, risk assessment, and sustainable treatment alternatives. J. Environ. Chem. Eng. 9 (5), 105966. https://doi.org/10.1016/j.jece.2021.105966.
Pastorino, P., Ginebreda, A., 2021. Contaminants of emerging concern (CECs): Occurrence and fate in aquatic ecosystems. Int. J. Environ. Res. Publ. Health 18 (24). https://doi.org/10.3390/ijerph182413401. Article 24.
Petrie, B., Barden, R., Kasprzyk-Hordern, B., 2015. A review on emerging contaminants in wastewaters and the environment: current knowledge, understudied areas and recommendations for future monitoring. Water Res. 72, 3–27. https://doi.org/10.1016/j.watres.2014.08.053.
Prajapati, A., Narayan Vaidya, A., Kumar, A.R., 2022. Microplastic properties and their interaction with hydrophobic organic contaminants: a review. Environ. Sci. Pollut. Control Ser. 29 (33), 49490–49512. https://doi.org/10.1007/s11356-022-20723-y.
Ren, P., Dou, M., Wang, C., Li, G., Jia, R., 2020. Abundance and removal characteristics of microplastics at a wastewater treatment plant in Zhengzhou. Environ. Sci. Pollut. Control Ser. 27 (29), 36295–36305. https://doi.org/10.1007/s11356-020-09611-5.
Richard, H., Carpenter, E.J., Komada, T., Palmer, P.T., Rochman, C.M., 2019. Biofilm facilitates metal accumulation onto microplastics in estuarine waters. Sci. Total Environ. 683, 600–608. https://doi.org/10.1016/j.scitotenv.2019.04.331.
Roscher, L., Halbach, M., Nguyen, M.T., Hebeler, M., Luschtinetz, F., Scholz-Böttcher, B. M., Primpke, S., Gerdts, G., 2022. Microplastics in two German wastewater treatment plants: Year-long effluent analysis with FTIR and Py-GC/MS. Sci. Total Environ. 817. https://doi.org/10.1016/j.scitotenv.2021.152619.
Rout, P.R., Mohanty, A., Aastha, Sharma, A., Miglani, M., Liu, D., Varjani, S., 2022. Micro- and nanoplastics removal mechanisms in wastewater treatment plants: a review. J. Hazard. Mater. Adv. 6, 100070. https://doi.org/10.1016/j.hazadv.2022.100070.
Rummel, C.D., Jahnke, A., Gorokhova, E., Kühnel, D., Schmitt-Jansen, M., 2017. Impacts of biofilm formation on the fate and potential effects of microplastics in the aquatic environment. Environ. Sci. Technol. Lett. 4 (3), 85–90. https://doi.org/10.1021/acs.estlett.7b00164.
Shi, X., Chen, Z., Wei, W., Chen, J., Ni, B.-J., 2023. Toxicity of micro/nanoplastics in the environment: roles of plastisphere and eco-corona. Soil & Environmental Health 1 (1), 100002. https://doi.org/10.1016/j.seh.2023.100002.
Singh, B., Sharma, N., 2008. Mechanistic implications of plastic degradation. Polym. Degrad. Stabil. 93 (3), 561–584. https://doi.org/10.1016/j.polymdegradstab.2007.11.008.
Stroski, K.M., 2019. Wastewater Sources of Priority Contaminants in Four Canadian Arctic Communities.
Schvartz, M., et al., 2023. Role of the protein corona in the colloidal behavior of microplastics. Environmental Science & Technology 57 (21), 16060–16071. https://doi.org/10.1021/acs.est.3c01515.
Schwabl, P., Köppel, S., Königshofer, P., Bucsics, T., Trauner, M., Reiberger, T., Liebmann, B., 2019. Detection of various microplastics in human stool: evidence for exposure to humans. Ann. Intern. Med. 171 (7), 453–457. https://doi.org/10.7326/M19-0618.
Stabnikova, O., Stabnikov, V., Marinin, A., Klavins, M., Vaseashta, A., 2022. The role of microplastics biofilm in accumulation of trace metals in aquatic environments. World J. Microbiol. Biotechnol. 38 (7). https://doi.org/10.1007/s11274-022-03293-6. Article 117.
Tasselli, S., Guzzella, L., 2020. Polycyclic musk fragrances (PMFs) in wastewater and activated sludge: analytical protocol and application to a real case study. Environ. Sci. Pollut. Control Ser. 27 (25), 30977–30986. https://doi.org/10.1007/s11356-019-06767-7.
Teuten, E.L., Rowland, S.J., Galloway, T.S., Thompson, R.C., 2007. Potential for plastics to transport hydrophobic contaminants. Environ. Sci. Technol. 41 (22), 7759–7764. https://doi.org/10.1021/es071737s.
Titov, I., Semerád, J., Boháčková, J., Beneš, H., Cajthaml, T., 2024. Microplastics meet micropollutants in a central European river stream: adsorption of pollutants to microplastics under environmentally relevant conditions. Environ. Pollut. 360, 124616. https://doi.org/10.1016/j.envpol.2024.124616.
Triebskorn, R., Braunbeck, T., Grummt, T., Hanslik, L., Huppertsberg, S., Jekel, M., Knepper, T.P., Krais, S., Müller, Y.K., Pittroff, M., Ruhl, A.S., Schmieg, H., Schür, C., Strobel, C., Wagner, M., Zumbülte, N., Köhler, H.R., 2019. Relevance of nano- and microplastics for freshwater ecosystems: a critical review. TrAC, Trends Anal. Chem. 110, 375–392. https://doi.org/10.1016/j.trac.2018.11.023.
UNEP, 2021. From pollution to solution: a global assessment of marine litter and plastic pollution. United Nations Environment Programme. https://www.unep.org/.
Wang, J., Liu, X., Li, Y., Powell, T., Wang, X., Wang, G., Zhang, P., 2019. Microplastics as contaminants in the soil environment: a mini-review. Sci. Total Environ. 691, 848–857. https://doi.org/10.1016/j.scitotenv.2019.07.209.
Wang, Y., Liu, C., Wang, F., Sun, Q., 2022. Behavior and mechanism of atrazine adsorption on pristine and aged microplastics in the aquatic environment: kinetic and thermodynamic studies. Chemosphere 292, 133425. https://doi.org/10.1016/j.chemosphere.2021.133425.
Yang, D., Shi, H., Li, L., Li, J., Jabeen, K., Kolandhasamy, P., 2015. Microplastic pollution in table salts from China. Environ. Sci. Technol. 49 (22), 13622–13627. https://doi.org/10.1021/acs.est.5b03163.
Yang, H., Chen, Z., Kong, L., Xing, H., Yang, Q., Wu, J., 2025. A review of eco-corona formation on micro/nanoplastics and its effects on stability, bioavailability, and toxicity. Water 17 (8), 1124. https://doi.org/10.3390/w17081124.
Zimmermann, L., Dierkes, G., Ternes, T.A., Völker, C., Wagner, M., 2019. Benchmarking the in vitro toxicity and chemical composition of plastic consumer products. Environ. Sci. Technol. 53 (19), 11467–11477. https://doi.org/10.1021/acs.est.9b02293.